Synchrotron X-ray fluorescence mapping of Ca, Sr and Zn at the neonatal line reflects changing perinatal physiology

M. Christopher Dean[1,2], Kathryn M. Spiers[3], Jan Garrevoet[3], Adeline Le Cabec[4],

[1]Department of Cell and Developmental Biology, University College London, Gower Street, London, WC1E 6BT, UK
[2]Department of Earth Sciences, Centre for Human Evolution Research, Natural History Museum, Cromwell Road, London SW7 5BD, UK
[3]Deutsches Elektronen-Synchrotron DESY, Notkestraße 85, 22607 Hamburg, Germany
[4]Department of Human Evolution, Max Planck Institute for Evolutionary Anthropology, Deutscher Platz 6, D-04103 Leipzig, Germany

Running title: Ca, Sr and Zn at the neonatal line

Declarations of Interest: none.

Author for correspondence:
Christopher Dean
Email: ucgacrd@ucl.ac.uk
Orcid.org/0000-0003-3783-7296

Abstract

Objectives: Our first objective was to review the evidence describing the appearance and microstructure of the neonatal line and to link this with known changes in neonatal physiology occurring at and around birth. A second objective was to explore ways to improve identification of the neonatal line by mapping the pre- and postnatal distribution of Ca, Sr and Zn in deciduous cuspal enamel and superimposing these maps onto transmitted light micrographs that included a clear true section of the neonatal line.
Materials and Methods: We used synchrotron X-ray fluorescence to map elemental distributions in pre- and postnatal enamel and dentine. Two deciduous canines and 5 molars were scanned with an X-ray beam monochromatised to 17.0 keV at either 10.0, 2.5 or 1.0 µm resolution and 10 ms integration time.
Results: Calcium maps distinguished enamel and dentine but did not clearly demarcate tissues formed pre- or postnatally. Strontium maps reflected presumed pre- and postnatal maternal serum levels and what are likely to be diet-dependent regions of Sr enrichment or depletion. Prenatal Zn maps, particularly for dentine, mirror elevated levels in the fetus and in colostrum during the first few days of life.
Conclusions: The neonatal line, enamel dentine junction and surface enamel were all Zn-rich. Within the neonatal line Zn may be associated with increased crystallinity but also with caries resistance, both of which have been reported previously. Elemental mapping may improve the identification of ambiguous NNLs and so be useful in forensic and archaeological studies.

Keywords: Deciduous teeth: Neonatal line: Prenatal enamel: Prenatal dentine: SRXF

Highlights

- The neonatal line forms when the neonate is both acidaemic and hypocalcaemic
- The neonatal line is not a consistently hypocalcified structure in exfoliated teeth
- The neonatal line and the deciduous cuspal EDJ are zinc-rich
- Elemental mapping may provide an additional way of identifying the neonatal line
- Trace elements in deciduous enamel reflect physiological and dietary shifts

1. Introduction

An accentuated marking, the neonatal line (NNL), forms at birth in teeth that begin to mineralise *in utero*. It is used in archaeology and palaeontology as a chronological marker of birth and in forensic science as evidence of a live birth. Yet its location, cause and duration are thought to be multifactorial. Rushton (1933) then Schour (1936) first identified the NNL in deciduous teeth and in the mesial cusp tips of first permanent molars. Schour studied 250 demineralised and 100 ground sections of deciduous teeth and found that 90% contained a NNL in the enamel and the dentine. In ground sections viewed with transmitted light microscopy (TLM), Schour (1936) noted prenatal enamel and dentine often stood out as brighter and more homogenous than darker postnatal enamel and dentine. Since demineralised prenatal dentine stained more heavily with hematoxylin and eosin, this suggested it was ‘better calcified’ (Schour, 1936; Kronfeld & Schour, 1939). Schour, (1936) also found the NNL in children with birth trauma to be ‘accentuated’, i.e. thicker and darker. In addition, Kronfeld & Schour (1939) noted that enamel appeared to be more sensitive than dentine to systemic disturbances.

In TLM of longitudinal ground sections of deciduous teeth, the NNL appears as a dark brown line or band. In enamel it is typically 10-30 μm wide (Kodaka et al., 1996) and runs obliquely from the enamel-dentine-junction (EDJ) towards the enamel surface. The precise location of the NNL within deciduous teeth varies according to gestation length and whether birth is preterm, term or post-term (Skinner & Dupras, 1993). Jakobsen (1975) also noted the NNL was confined almost exclusively to the mesiobuccal cusp of first permanent molars and occurred with a lower frequency in a sample of males than in females, where initiation of mineralisation is on average more advanced.

Within the NNL, Weber & Eisenmann (1971), demonstrated discontinuity of the prisms that appeared to be temporarily interrupted. In very thin ground sections (~4 μm) viewed with TLM this discontinuity consists of dark enamel cross striations that form a zig-zag or staircase arrangement within the NNL. With SEM, Whittaker & Richards (1978) also demonstrated a 0.2 μm interruption running transversely across some prisms within the NNL but cautioned that preparation or shrinkage artefact could not be excluded as contributing to this. Kurek et al. (2015) also noted that this interruption is not a consistent feature. In a sample of 50 deciduous teeth Whittaker & Richards (1978) noted considerable variation in the degree of prism width, constriction and deviation within the NNL. Others have also reported changes to the relative thickness of the prism boundaries within the NNL (Rushton, 1933; Sognnaes, 1949; Gustafson 1959; Gustafson & Gustafson, 1967; Kodaka & Higashi, 1995; Kodaka et al., 1996).

Microradiography has revealed the NNL to be relatively radiolucent suggesting it is hypomineralised (Crabb, 1959; Allan 1960; 1967; Silness, 1969; Kodaka et al., 1996; Sabel et al., 2008) although (Rushton, 1939) considered prisms within the NNL to be hypermineralised. Sabel et al. (2008) showed a clear gradient in mineral density with microradiography that was high at the EDJ and reduced towards the enamel surface in developing tooth germs. In these unerupted tooth germs the NNL was clearly radiolucent (hypomineralised). However, while this gradient seems well established in early maturing deciduous enamel, (Allan, 1959: Crabb, 1959), it may change with age as the outer enamel progressively attains higher levels of mineralisation through post-eruptive uptake of mineral from the oral environment (Wilson & Beynon, 1989). Again, based on microradiography (of extracted teeth), Mortimer (1970) concluded prenatal deciduous enamel had 3-4% lower mineral content than postnatal enamel but that the area surrounding the NNL was least mineralised with levels 2-3% lower than adjacent prenatal enamel. While microradiography reflects the radiodensity of total mineral content, it may not be a true reflection of Ca concentration.

Weber & Eisenmann (1971) identified prominent radiolucent prism boundaries and cross striations within the NNL but noted there was also a diffuse ~10 μm radiolucent zone either side of the NNL. They attributed this to decreased crystal concentration. Using SEM, Whittaker & Richards (1978) also noted a ~15 μm diffuse zone but only on the postnatal side of the NNL in which crystals appeared to be less tightly packed. Prominent prism boundaries and occasional irregularly shaped or fused prisms were identified within the NNL, in transverse section (Kodaka & Higashi, 1995; Kodaka et al., 1996). They further observed highly disordered crystallite arrangements yet which did not show low BSE signals. Kodaka et al., (1996) proposed that a temporary loss of the Tomes' process in response to ameloblast stress was responsible for this dysmorphology.

Ultrastructural transmission electron microscope (TEM) studies (Weber & Eisenmann, 1971) showed the NNL to consist of a thin 'crystal-deficient' region running a 'tortuous course obliquely across the enamel prism' (Weber & Eisenmann, 1971). Weber & Eisenmann (1971) further reported that, when present, these 'abnormal crystal patterns existed as scattered regions of decreased crystal concentration in proximity to the NNL' and that 'fine granular material was present in the spaces between the crystalline borders of pre- and postnatal enamel', (Weber & Eisenmann (1971).

Little has been reported regarding the chemistry of the NNL itself but Sabel et al. (2008) made SEM X-ray Micro Analysis (XRMA) measurements of Ca, P, K, Mg and Na perpendicular to the NNL in the enamel of an exfoliated tooth. Ca, P and Ca/P were constant through pre- and postnatal enamel although K, Na and Mg each gradually decreased. However, distinctly lower values for both Na and Mg were coincident with the NNL.

A number of studies have used laser ablation inductively coupled plasma mass spectrometry (LA-ICP-MS) to sample trace elements normalized to Ca in enamel either side of the NNL. Lochner et al. (1999) and Dolphin et al. (2005) reported a rise in almost all trace elements after birth, including Zn. An exception was Mg/Ca that reduced postnatally and Sr/Ca that was bimodal, either remaining the same or rising in one group or falling to lower postnatal levels in a second group. Müller et al. (2019) have further investigated underlying trends through pre- and postnatal enamel using LA-ICP-MS and observed a 30-80% decrease in Sr/Ca from the EDJ to the surface enamel that they attributed to the several-fold upregulation of Ca metabolism and active transport of Ca through ameloblasts during enamel maturation. Humphrey et al. (2004; 2007) also used LA-ICP-MS to sample trace elements in enamel either side of the NNL. Superimposed upon an underlying trend, they observed a pattern of change in the Sr/Ca ratio across the NNL that was consistent with a model based on physiological concentrations of Ca and Sr resulting from ongoing maturation of the digestive tract and shifts in diet during deciduous enamel formation (Humphrey et al., 2004; 2007; 2008b; 2008c). However, the chemistry of the NNL itself and any abrupt boundary changes co-incident with its microstructure remains unclear.

There is general agreement that the physiological changes occurring at birth are in some way responsible for the presence of the NNL but it remains less clear what specifically underlies its microscopic appearance. Sabel et al. (2008) noted that infants are born acidaemic, as is the case in most mammals examined (Krukowski & Smith, 1976). Stenger at al. (1964) reported differences in O_2 tension between mother and fetus but also between infants delivered by 'complicated' or 'uncomplicated' Caesarean section. Bakker et al. (2007) reported increased uterine activity (shorter relaxation time) during the first and second stage of labour is associated with an increased incidence of lower pH values (~7.1) in the umbilical artery at birth. Helwig et al. (1996) recorded umbilical arterial and venous pH, pCO_2 and pO_2 values within 5 minutes of birth in 15,073 infants with an Apgar score ≥ 7. Mean umbilical artery pH was 7.26 (2.5^{th} – 97.5^{th} percentile range 7.10-7.38) compared with the normal postnatal arterial blood pH of 7.35-7.45. They noted that infants born by Caesarean section or operative vaginal delivery were more acidaemic than those born by normal spontaneous vaginal delivery and that small but significant differences also existed between preterm, term and post-term infants. However, these very small differences in mean pH varied only by 0.02 or 0.03 pH units (Helwig et al. 1996). Nonetheless, Okada (1943) has previously demonstrated the effects of minor fluctuations in acid base balance on the formation of light and dark incremental growth lines and parturition lines in enamel and dentine.

As infants begin to breath at birth and blow off CO_2, both pO_2 levels and pH levels rise (Krukowski & Smith, 1976). Fetal serum calcium levels are higher than maternal

levels with a 1:1.4 maternal to fetal Ca gradient (Hsu & Levine, 2004; Kovacs, 2011). This may in part be maintained by the prenatal acidaemia (Krukowski & Smith, 1976). However, active transport of Ca and P across the placenta ceases at birth and blood pH rises, normally within hours. As a result, serum Ca levels fall to a low point within 24-48 hours of birth, in response to which the immature parathyroid glands begin to function (Krukowski & Smith, 1976; Hohenauer et al. 1970; Meites, 1975; Hsu & Levine, 2004; Kovacs, 2011). While postnatal Ca levels range between 2.2-2.7 mmol/L they maybe 1.2 ± 0.02 mmol/L on day 1 after birth (Ranggard et al. 1994). Persistent, or late onset hypocalcaemia, may result from dietary hyperphosphatemia or from neonatal vitamin D deficiency as maternally derived stores become depleted and there is increased reliance on vitamin D-dependent transport of Ca across the gut (Hsu & Levine, 2004). Gittleman et al. (1956) reported that the incidence of postnatal hypocalcaemia was greater in infants delivered by Caesarean section and premature infants than in full-term infants delivered vaginally. Additionally, Colak et al. (2014) found a correlation between cord blood Ca and P levels and birth size parameters.

The combination of low serum Ca levels and low pH at birth seems an obvious likely underlying cause of NNL formation and appearance. However, Ranggard et al. (1994) measured the width of the NNL in 24 teeth from infants where ionized blood Ca levels had been recorded on days 1, 3 and 5 postpartum and found comparatively thin NNLs (5 μm or less) in all teeth and no correlation between NNL width and blood Ca levels.

Width of the NNL has been used as an indicator of the period of physiological stress at birth. However, Kodaka et al. (1996) noted that both NNL width and opacity varied in TLM and microradiographs of the same tooth. Moreover, Weber & Eisenmann (1971) demonstrated that NNL width is difficult to standardise. Both plane of section and section obliquity each have a considerable effect on measurements of NNL thickness (Weber & Eisenmann, 1971; Jakobsen, 1975; Canturk et al., 2014). In ground sections and in microradiographs NNL width reduces as section thickness reduces (Weber & Eisenmann, 1971). Nonetheless, Eli et al. (1989) and Canturk et al. (2014) reported that NNL width is thinner in infants born by Caesarean section and wider in infants born by difficult operative delivery. Hurnanen et al. (2017), on the other hand, found a highly significant correlation between NNL width and duration of vaginal deliveries but, perhaps counterintuitively, NNL width was narrower where the duration of delivery was longer. Interestingly, Zanolli et al. (2011) found factors related to gestational length rather than mode of delivery may have some influence of NNL thickness and Kurek et al. (2005) observed that infants of mothers who took antispasmodic smooth muscle relaxants had thinner NNLs and further observed that infants born in the Spring and Summer had thinner NNLs than those born in Winter. Żądzińska et al. (2013) found that birth in the Spring and Summer was also associated with thinner prenatal (but not postnatal) enamel thickness, which they tentatively attributed to an underlying prenatal vitamin D deficit and its effect on ameloblast and odontoblast matrix secretion recovery rate at birth. However, Keinan et al. (2007; 2007) also reported thicker and more highly mineralised prenatal enamel in deciduous canines (but exactly the converse in deciduous second molars) in Down's syndrome children emphasising the crucial role of timing during dental development *in utero*.

NNL formation is clearly complex and multifactorial. The aim of this study was to use Synchrotron X-ray Fluorescence (SXRF) to map the Ca, Sr and Zn concentrations in pre- and postnatal enamel and dentine and identify any boundary shifts in chemical composition occurring at the NNL in a sample of naturally shed deciduous teeth. It is generally accepted that the physiological stress of the birth process underlies the appearance and structure of the NNL. However, establishing a clearer link between changing perinatal physiology, the mineralisation process and the trace element composition of enamel and dentine at this time may improve our understanding of NNL formation, microstructure and appearance. Moreover, identifying the NNL in forensic and archaeological studies can be difficult such that any additional evidence that may enable this is of practical importance.

1. Materials and methods

Twelve naturally shed modern human deciduous teeth that had been stored dry for between 30 and 40 years were then donated with consent for study. No personal data were collected, recorded or stored as part of this study. Teeth were sectioned longitudinally with a low speed diamond saw (*Buehler IsoMet*). One cut face was polished using a graded series of abrasive papers and finished with 3 μm aluminium polishing powder and deionised water on a polishing pad. This polished surface was cleaned in an ultrasonic bath, dried and then fixed to a 1 mm thick glass slide with zero-bond epoxy resin (*Huntsman Araldite 2020*) under pressure for 48 hours. A further cut was then made parallel with the glass slide and tooth block leaving a 300-400 μm thick longitudinal tooth section attached to the slide. This was then ground and lapped to between 80-100 μm and polished. No coverslip was placed leaving the polished surface exposed for SXRF. From this original sample of twelve teeth, 2 deciduous canines and 5 second molars, were selected for use in this study on the basis that the NNL was easily visible in TLM and showed no section obliquity. Two teeth, a canine and second molar, were chosen from the same individual so that the elemental distributions and NNL morphology in each tooth might be compared and cross-matched.

Experiments were performed on the Beamline P06 (Schroer et al. 2010; Boesenberg et al., 2016), Petra III, at DESY (Deutsches Elektronen-Synchrotron, a member of the Helmholtz Association HGF), Hamburg, Germany. The storage ring was operated in 40-bunch mode using top-up filling mode with a current of 100 mA ± 0.5 mA. The primary X-ray beam was monochromatised to 17.0 keV using a double crystal Si111 monochromator and focused using a Kirkpatrick-Baez (KB) mirror system (JTEC, Japan) to 0.5 × 0.5 μm. The focused X-ray beam decreases any background signal, thus improving trace element sensitivity, effectively reducing the needed radiation dose (Sun et al., 2015). For this experiment, the set-up comprises a Maia detector system (Kirkham et al. ,2010), which allows for large area SXRF imaging with a sub-micrometer resolution using millisecond dwell times (Falkenberg et al. 2017). The Maia detector is ideal for use in 180° or “backscatter” geometry of thin polished samples (~100 μm-thick in this study). The sample is placed perpendicular to the incident X-ray beam, and positioned beyond the Maia detector (see figure 2 in Sun et al. 2015). The Maia Si detector wafer comprises 384 diode elements, each 1 mm^2, arranged in a 20 × 20 array, with 4 × 4 elements missing in the centre of the detector. This leaves a central hole through which the incident beam passes. This set up, combined with a sample position very close to the

detector, results in the detector wafer subtending a sample solid angle of approximately 1.3 sr. The sample holder supporting the sample is fixed to a sample stage using a kinematic mount (Newport). Data is acquired in 'flyscanning' mode by continuously moving the sample relative to the X-ray beam. Elements of primary interest were Ca, Sr, and Zn therefore the primary energy of 17.0 keV was chosen, sufficient to excite the Sr K-shell but not the Mo mask in the Maia detector. Spectral analysis, deconvolution and initial image analysis of the fluorescence data were performed using GeoPIXE 7.4f. Elemental distribution maps were normalised to the incoming X-ray flux. SXRF concentrations are reported as ppm (by weight).

Lower resolution overview scans were first acquired with a resolution of 10 μm, and an integration time of 10 ms (Fig. 1). Scan times for these were typically between 1.3 and 2.5 hours depending on tooth size. The cuspal region containing the NNL in two further deciduous second molars were scanned at higher resolution, 2.5 μm, 10 ms, scan times 2.1 and 1.0 hours respectively, (Fig. 2). Finally, the NNL in the enamel and dentine at the EDJ was scanned in two additonal teeth, a deciduous second molar and a canine, at 1 μm, 10 ms integration times for which scan times were 50 mins and 43 mins (Figs. 3 & 4).

2. Results

The SXRF Ca overview maps (Fig. 1) show a marked contrast between enamel and dentine that reflects their different levels of calcification. No obvious directional Ca gradients were observed within enamel or dentine. The overview Sr maps also show higher levels in enamel than dentine, again reflecting relative mineralisation levels. Strontium levels varied through dentine formation. In all three deciduous teeth early forming dentine in the cusps showed lower levels of Sr compared to later formed dentine towards the cervix and root (Fig. 1). A prominent Sr band in one second deciduous molar and two matching Sr bands in the canine and molar from the same individual mark the start of a shift to Sr enrichment at approximately 10 -12 months into tooth formation (Fig. 1). The distribution of Zn is similar in all teeth with a zone of enrichment at the outer surface enamel, in the cementum and secondary dentine. There is also Zn enrichment in the prenatal dentine and at the NNL.

Higher resolution SXRF maps of the NNL in an upper deciduous second molar (Fig. 2a-d) and a lower second deciduous molar cusp (Fig. 2e-h) show little evidence of a difference in pre- and postnatal enamel Ca fluorescence intensity. While the NNL in enamel appears minimally hypercalcified in the canine (Fig. 2b), it is hypocalcified in the molar (Fig. 2f). A halo of Sr enrichment exists in the prenatal enamel of both cusps that is bounded by the NNL but this is imperceptible in prenatal dentine (Fig. 2c,g). In both the canine and molar cusp the NNL is Zn-rich (Fig. 2d,h). While prenatal dentine is also relatively Zn-rich there is no evidence for this in prenatal enamel. High levels of Zn, presumed to be within the dentine tubules, run through both pre- and postnatal dentine. In the molar cusp (Fig. 2h), the surface enamel is Zn-rich except where the tooth surface has worn away in function.

A further deciduous molar and canine (additional to those illustrated in Figs. 1 & 2) were scanned at 1 μm resolution where the NNLs in enamel and dentine converge towards the EDJ. The NNL is imperceptible in the Ca SXRF maps of enamel and dentine (Figs. 3 & 4) although prenatal dentine can just be demarcated from

postnatal dentine (Fig. 3). It is not possible to be certain whether the apparent Ca enrichment along the enamel EDJ might result from an edge effect but this is less apparent in the dentine at the EDJ. The NNL and the EDJ (again with the possibility that there is an edge effect at the EDJ) are Zn-rich. Evidence of dentine tubule morphology in the Ca and Zn maps may result from hypercalcified and Zn-rich peritubular dentine contrasting with the inter-tubular dentine. Neither of the 1 μm resolution maps of these two deciduous canines show any clear evidence of enamel prism morphology. In the Sr maps the prenatal enamel is enriched relative to the postnatal enamel. In dentine, only the NNL in one of the canines shows any evidence of Sr enrichment (Figs. 3 & 4).

The profile and elemental concentration plot (Fig. 5) made through the upper deciduous second molar cusp tip (also depicted in Fig. 2e-h) quantifies the Zn and Sr distribution through pre- and postnatal enamel and dentine. Zinc concentrations in enamel are close to zero but rise to ~200 ppm at the NNL. Zinc levels in prenatal dentine fluctuate between 150 and 250 ppm, thus exceeding those in enamel but rise to ~300 ppm at the NNL in dentine. Small peaks in Zn concentration coincide with dentine tubule profiles and may reflect high levels of Zn in peritubular dentine. Strontium levels appear consistently higher in pre- and postnatal enamel (~150 ppm) than in pre- and postnatal dentine (~100 ppm). A halo of Sr enrichment (~160 ppm) around the cusp tip in prenatal enamel falls to below 150 ppm beyond the NNL in postnatal enamel.

Two concentration profiles are shown through the lower second deciduous molar cusp (Fig. 6a,b). Both show a similar distribution pattern for Zn and Sr as the canine cusp (Fig. 5). Zinc concentration is higher in dentine than in enamel. At the NNL, Zn levels in dentine are also higher than in enamel (150-200 ppm). In enamel, Zn concentration is close to zero in inner enamel but shows a slight rise at the NNL to ~25 ppm. Towards the enamel surface Zn concentration rises steeply to ~400 ppm (Fig. 6a). As in the upper deciduous second molar cusp (Fig. 5), the pattern of Sr distribution across enamel and dentine is reversed with respect to Zn and Sr levels in dentine (~120 ppm) are lower than those in enamel (~160 ppm). Evidence of a reduction in Sr concentration from pre- to postnatal enamel is less clear in this molar cusp.

3. Discussion

The NNL is an important marker of birth in forensic science (Jakobsen, 1975; Janardhanan et al., 2011; Witzel, 2014) and in archaeological science (Macchiarelli & Bondioli, 2000; Zanolli et al., 2011; Hillson, 2014; Birch & Dean, 2014; Nava et al., 2017; 2019) as well as being of some clinical significance (Mishra et al., 2004). Within the small sample of deciduous teeth chosen for this study the appearance of the NNL viewed with non-polarised TLM varied greatly both in width and morphology (Fig. 7). Notably, prisms appeared either to have an irregular path through the NNL, or not, and the quality of the pre- and postnatal enamel appeared either different or alternatively quite similar. Even within a single tooth section, images of the NNL in the cuspal region (Fig. 7a) and close to the EDJ (Fig. 7c) varied considerably. Besides the obvious issues of section obliquity and section thickness, this raises other issues of how ameloblasts and odontoblasts in different locations and of different secretory age might respond differently to the physiological changes

occurring around birth. Figure 7d also illustrates a further problem, previously discussed and illustrated by Jakobsen (1975), of how difficult it can be to distinguish the NNL from other forms of accentuated incremental marking in enamel and dentine when both occur close together.

Thomas & Lee (2003) noted the NNL appeared to deflect the progress of caries laterally along the plane of the NNL rather than continuing inwards into prenatal enamel. Mishra et al. (2008) measured rates of demineralisation in pre- and postnatal enamel using scanning microradiography and concluded this was no different, even though previous studies have reported differences in the degree of mineralisation between these (Mortimer, 1970; Wilson & Beynon, 1989). Within the region of the NNL, however, rates of demineralisation were much lower, again, despite previous evidence that the NNL is hypomineralised (Crabb, 1959; Allan 1960; 1967; Silness, 1969; Sabel et al., 2008). One explanation given for this was that slower enamel formation at the NNL would reduce the carbonate-plus-magnesium ratio to calcium-plus-phosphate, rendering the mineral phase inherently less acid soluble (Mishra et al., 2008). Another explanation was that some 'inhibitory impurity' might accumulate in the NNL during development (Mishra et al., 2008). Other potential barriers to caries progression exist in teeth, such as the spatial arrangement of hydroxyapatite crystals that are highly aligned in caries-resistant enamel (Johnson et al. 1971; Cevec et al., 1980; Skaleric et al., 1982). Yet, given the findings of previous studies (Weber & Eisenmann, 1971; Kodaka & Higashi, 1995), this would seem an unlikely structural characteristic of the NNL. In the small sample of deciduous teeth used in this study, there was no clear demarcation in calcium concentration between pre- and postnatal enamel or dentine nor was there a consistently hyper- or hypocalcified NNL. Very few deciduous teeth were included in this study, however, this might suggest that within limits, ameloblasts and odontoblasts are able to buffer the effects of higher Ca levels prenatally. On the face of it, the results of this study differ from those of Schour, (1936) and Kronfeld & Schour, (1939) who interpreted brighter, more homogenous prenatal enamel viewed in TLM as better calcified. A cautionary observation here would be that all teeth in this study had been in function within the oral environment for more than 10 years and newly erupted or unerupted deciduous teeth might present a different picture.

4.1 *Zinc in enamel and dentine*

Zinc is an abundant trace element that is required for cell division and tissue growth. It plays a key role in embryogenesis and fetal development (Ezzo, 1994; Donangelo & King, 2012). Zinc is not only required for the DNA binding proteins involved in regulating gene expression but is also a component of many metalloproteins and enzymes, besides being involved in most major metabolic pathways (Terrin et al., 2015). It has previously been suggested that Zn levels in dental tissues are elevated in outer enamel, secondary dentine, peritubular dentine and cementum because there is prolonged direct contact with tissue fluid during their formation (Sánchez-Quevedo et al., 1992; Martin et al., 2007; Stock et al., 2011; 2014; 2017; Dean et al., 2018). A zinc finger-containing transcription factor, Osterix (*Osx*), is expressed in differentiating coronal odontoblasts at early postnatal periods (Kim et al., 2015), which raises the question as to whether Zn enrichment observed at the cuspal EDJ (Fig. 2 d,h; Figs. 3 & 4) might be residual to that involved with this early regulatory mechanism.

Maternal serum Zn levels decline 15-35% by late pregnancy to around 48.5 ± 17.6 µg/dL but remain high in cord blood as Zn is actively transported across the placenta and transferred to the fetus (Dreosti et al., 1982; Wasowicz et al. 2001; Ofakunrin et al., 2017). In the last trimester, Zn levels in the fetus increase to around 99.3 ± 21.5 µg/dL and are maintained at constantly higher than maternal levels (Terrin et al., 2015; Ofakunrin et al., 2017). Zinc is critical for lactation and levels in colostrum on days 1-4 postpartum are high (7.99 ± 3.23 mg/L) but falling to less than half that within a week (Silvestre et al., 2001; Wasowicz et al., 2001). During the first days of lactation high levels of Zn are excreted to milk from maternal blood irrespective of dietary intake and Wasowicz et al. (2001) reported the milk/plasma ratio of Zn during the first 4 days postpartum to be 16.1 mg/L.

This evidence suggests there is reason to expect higher Zn levels in prenatal than postnatal dentine (Figs. 4 & 5). For an infant breast-fed at birth, even higher levels of Zn might be incorporated into enamel and dentine mineralising during the immediate postnatal period. Peritubular dentine contains no collagen and besides containing smaller hydroxyapatite crystals, the mineral component also contains amorphous calcium phosphates as well as tricalcium and octacalcium phosphate (Berkovitz et al., 1981; Bodier-Houllié et al., 1998). Interestingly, the formation of these mineral components is promoted or stabilised by the presence of Zn (LeGeros et al., 1999). Stock et al. (2011; 2014; 2017) previously found that Zn signals in peritubular dentine peaked at 2.4 to 3.2 times that in inter-tubular dentine. Some evidence of this can be seen in this study (Figs. 2 & 5) where bright streaks following dentine tubules are likely to represent Zn rich peritubular dentine. Stock et al. (2017) have argued that Zn levels are elevated where there is active mineralisation, as there is throughout life in peritubular dentine, and that while some Zn is transient, some may remain sequestered in the tissue. Zinc interacts with hydroxyapatite formation and influences crystallite growth. It is also reported to reduce crystallinity (LeGeros, 1981; LeGeros et al., 1999) and enamel acid dissolution (Weber and Eisenmann, 1971; Featherstone et al., 1980; Mayer et al., 1994; Mishra et al., 2008; Lingawi et al., 2011).

When Zn is present at concentrations greater than 107 ppm, and at low pH (~4.0), it is actively involved in a dissolution / reprecipitation reaction where a new mineral phase (alpha-hopeite, alpha-$Zn_3(PO_4)_2H_2O$) forms on the hydroxyapatite lattice surface, so blocking further demineralisation (Mohammed et al., 2014). Given that both reduced enamel dissolution and altered crystallinity have been observed at the NNL, the evidence for Zn distribution in this study (Figs. 2-5) suggests that Zn may well be the ‘inhibitory impurity’ at the NNL proposed by Mishra et al. (2008) and that this directly reflects changing pre- and postnatal Zn levels. The results of this study do not support the earlier more general findings of Lochner et al. (1999) and Dolphin et al. (2005) who reported a postnatal rise in Zn/Ca.

Besides the perinatal distribution of Zn in the region of the NNL, Zn concentration increases towards the enamel surface (Figs. 1 & 6). Zinc enrichment at the enamel surface has been documented previously using LA-ICP-MS (Humphrey et al., 2008a; Müller et al., 2019). Müller et al. (2019) observed Zn/Ca ratios increased near-exponentially some 20-35 times towards outer enamel. Zinc exchange from the post-eruptive oral environment may well contribute to this surface enrichment (Humphrey et al. 2008a) but it is notable in this study that worn enamel, despite having being

exposed to saliva, is not Zn rich. Zinc at the enamel surface has also been tentatively linked to the intense involvement of Zn in the process of enamel mineralisation and maturation (Humphrey et al. 2008a; Klimuszko et al., 2018; Müller et al., 2019).

Enamel crystallites begin to form within 24 hours of enamel matrix secretion (Boyde, 1964; 1989). These initially formed 'young' crystallites are Mg and carbonate rich and eventually become the central portions of the adult enamel crystallites (Boyde, 1997). Rosser et al. (1967) used scanning electron-probe X-ray emission microanalysis to quantify increasing Ca concentration in the enamel of human third molars. They calculated this to be linear with distance from the developing surface at 2.7% per μm reaching over 90% in inner enamel prior to cessation of enamel matrix secretion at the enamel surface. Simmons et al. (2013) have demonstrated that the rate of mineral formation and of mineral organisation are not, however, identical with crystallite organisation continuing for much longer. Crystallites quickly extend in length along their c-axes guided by ribbon like scaffolds made up of self-assembling amelogenin nanospheres (Du et al., 2005). Growth in crystallite width and thickness (a- and b-axes) is, however, prevented by matrix proteins that occupy the spaces between crystal ribbons (Lu et al., 2008). Robinson et al. (1997) observed that carbonate both retards crystal growth and promotes specific growth in crystal width compared with thickness. However, secretory stage ameloblasts also secrete a protease, matrix metalloproteinase 20 (MMP-20, also known as enamelysin) that slowly cleaves and degrades amelogenin and other enamel proteins. This enables slow and controlled thickening of the crystallites during the secretory stage that pack increasingly tightly together within in the deeper enamel and may also fuse together (Robinson et al. 1997; Al-Mosawi et al., 2018). MMP-20 contains Zn some of which may conceivably be retained in deeper enamel after proteins are degraded depending on the efficiency with which they may, or may not, be removed from the matrix during the secretory stage (Müller et al., 2019). There is an ongoing bi-directional gradient of enamel mineralisation from the EDJ to the surface enamel and from the cusp tip cervically (Al-Mosawi et al., 2018).

At the end of the secretory stage, growth in enamel crystallite length ceases although Rosser et al. (1967) reported there is no second, sudden increase in mineral content. Simmons et al. (2013) have emphasised that the precise timing of the various formation and maturational phases of enamel formation in humans remains vague. Transitional and maturational ameloblasts now secrete a more aggressive serine protease, kallikrein 4 (KLK4) into the extracellular space. This cleaves and degrades virtually all remaining organic matrix surrounding crystallites including amelogenin and enamelin (Lu et al., 2008). But continuing crystal growth releases protons (H+) that lower the pH of the extracellular compartment and inhibit, and/or possibly control, crystallite growth (Robinson, 2014). Ameloblasts, through the action of carbonic anhydrase on CO_2 and H_2O, then secrete bicarbonate into the extracellular space to buffer this, so lowering pH and favouring hydroxyapatite crystal growth (Lacruz et al., 2009; Robinson, 2014).

Zinc reaches highest levels in the ameloblast nucleus during enamel maturation and Zn a component of alkaline phosphatase, of carbonic anhydrase, of MMP-20 and KLK4 (Klimuszko et al., 2018). Zinc is also a potent inhibitor of serine proteases including KLK4 and so may act to modulate enamel protein degradation. For these

reasons it has been suggested Zn enrichment, especially of the outer enamel (Figs. 1 & 6), might result from the retention of Zn originally involved in the enamel mineralisation and maturation process. Greater amounts of Zn are involved in enamel maturation and so more may be retained in the outer enamel than in inner enamel. Robinson et al. (1997), however, have observed that during the final maturation phase there is relatively free access of diffusible ions (such as Mg) into the enamel and it may well be that relatively free diffusion of Zn ions during maturation contributes to the Zn-rich surface enamel layer. Surface exchange from Zn present in the diet and the oral environment will also surely accumulate at the enamel surface of teeth examined many years post-eruption such as those included in this study (Klimuszko et al., 2018; Müller et al., 2019; Humphrey et al., 2008a).

4.2 *Strontium in enamel and dentine*

Calcium and P are actively transported across the placenta (Hohenauer et al., 1970; Meites, 1975; Hsu & Levine, 2003; Kovacs, 2011) and Ca is also actively transported across the mammary gland (Neville & Watters, 1983). However, Sr (as well as Li and Mo) are not actively transported across the mammary gland but rather follow a physiological concentration gradient (Rossipal et al., 2000). Strontium also seems likely to be incorporated into dental hard tissues in a manner that reflects its changing physiological concentrations within the interstitial tissue fluid adjacent to the odontoblasts and ameloblasts (Humphrey et al., 2004; 2007; 2008b; 2008c; Müller et al., 2019). Strontium concentrations also depend upon the degree to which a series of metabolic processes discriminate against or favour Sr relative to Ca (Ezzo, 1994; Humphrey et. al., 2007; 2008c; Humphrey, 2009; 2014). Strontium discrimination occurs with respect to Ca in the intestine, kidney, placenta and mammary gland (Ezzo, 1994). In particular Ezzo (1994) pointed out that if 10-14% of ingested Ca is passed to milk via the mammary gland then only 1% of ingested Sr is passed to milk. In infants who are breastfed this reduction in physiological interstitial Sr available to ameloblasts and odontoblasts will be reflected in the composition of mineralising dental tissues (Humphrey et al., 2004; 2007; 2008b; 2008c; Humphrey 2009; 2014). These observations explain why the proportion of Sr to Ca incorporated into the enamel and dentine of a breastfed infant is likely to be reduced at birth until such time as dietary Sr is introduced, as either a breast milk formula supplement or as a complete replacement for breast milk at weaning (Humphrey et al. Humphrey, 2009). They more than likely explain the halo of Sr rich prenatal enamel (Figs. 5 & 6) that appears to end abruptly at the NNL and also the pattern of Sr enrichment in enamel and dentine ~10 to 12 months into tooth formation (Fig. 1) at a time when cessation of breastfeeding and weaning onto a diet containing Sr often takes place.

The greatest difference in Sr concentration observed in this study was between enamel and dentine (Figs. 5 & 6). Apart from a slight peak in prenatal enamel and small fluctuations due to shrinkage cracks in the tooth section, Sr concentration is remarkably stable in both enamel and dentine (Figs. 5 & 6).

In forming dentine, Ca is actively transported transcellularly from the pulp interstitial fluid to the extracellular dentine matrix and significant levels of alkaline phosphatase and Ca-ATPase have been localised in the membrane vesicles and Golgi within the odontoblasts processes (Granstrom & Linde, 1981; Bawden, 1989). Mineral laid down during dentine mineralisation will, therefore, more than likely have a greater

proportion of Ca/Sr than exists physiologically in the interstitial fluid. It follows the difference in Sr concentration between enamel and dentine (Figs. 5 & 6) results largely from dentine being generally less well mineralised than enamel. However, the proportion of Sr/Ca in dentine may also be lower because Ca is actively transported to the mineralising dentine front at the expense of Sr that can be assumed only to follow a physiological concentration gradient. This may explain why, in contrast to enamel, no obvious change in Sr concentration is detectable at the NNL in dentine (Figs. 5 & 6).

During the early secretory stage of enamel formation only low and stable concentrations of Ca are required for crystallite growth and both Ca and Sr are thought to diffuse passively across the ameloblast cell layer (Bawden, 1989; Humphrey et al., 2004; 2007; 2008b; 2008c). Indeed, Ca may even be actively removed from the intra- and extracellular ameloblast space to maintain optimally low concentrations for this to occur (Bawden, 1989; Hubbard, 2000; Humphrey et al. 2008c). However, a three- to four-fold increase in demand for Ca occurs during the later maturational stage of enamel formation and requires active transcellular transport of Ca^{2+} into the extracellular enamel space (Bawden, 1989; Hubbard, 2000). Within maturational amelobalsts specific CaATPase pumps are involved in the active transport of Ca^{2+} ions. This increase in Ca transport, together with Sr continuing to follow a physiological concentration gradient into the ameloblast extracellular space, underlies the reduction in Sr/Ca towards the enamel surface observed by Humphrey et al. (2004; 2007; 2008b; 2008c) and Müller et al. (2019). The finding in this study that Sr concentration remains unchanged, even close to the enamel surface (Fig. 6) where the maturation process and active Ca transport is most intense, is compatible with this scenario but also implies dietary intake and absorption of Sr remained unchanged during deciduous cuspal enamel formation.

5. **Conclusions**

The SXRF maps of Ca, Sr and Zn presented in this study allow us to make a clearer link between some of the physiological events that occur around birth and the chemistry of mineralising enamel and dentine. The results do not support the view that prenatal enamel is uniformly better calcified than postnatal enamel. They do, however, support previous findings about the distribution of Sr in pre- and postnatal enamel. Our findings provide new evidence for increased levels of Zn in prenatal enamel and dentine and for Zn enrichment at the EDJ and within the NNL itself. The data presented here provide a supplementary line of evidence for identifying the NNL more securely by linking its microstructural appearance with a potential boundary line demarcating shifts in pre- and postnatal Sr and/or Zn levels. This may be particularly pertinent for forensic studies that rely on the presence of the NNL for evidence of a live birth. Overall, the results offer only limited support for the view that the NNL is simply a hypocalcified (or in a more general sense hypomineralised) accentuated marking. Rather, they support previous studies that have proposed a region of reduced and disordered crystallinity, at least in enamel, that results in light scattering properties that give the typically dark brown NNL seen in TLM and light blue NNL appearance seen in reflected light microscopy (Boyde, 1964; 1989). A surprising finding is the precise demarcation of Zn and Sr distribution at the NNL in the enamel of some teeth that suggests minimal temporal overprinting of these trace elements.

Conflict of Interest

The authors declare no conflict of interest. All authors have read and approved the final article.

Ethics statement

All work carried was exempt from any requirements set out in The Code of Ethics of the World Medical Association (Declaration of Helsinki).

Acknowledgements

All preparatory lab work was carried out at UCL and on collections based there. All experimental work was carried out at the DESY synchrotron in Hamburg (Deutsches Elektronen-Synchrotron, a member of the Helmholtz Association HGF) on the PETRA III P06 beamline. The work presented in this study was supported by DESY Project proposal I-20160686 and Project proposal; I-20180047. We thank the DESY User Office, Dr. Gerald Falkenberg and those who have developed techniques employed in this study. We acknowledge support to CD from the Calleva Foundation and to ALC from The Max Planck Society. We thank Jean-Jacques Hublin for continuing support with this project.

References

Allan, J. H. (1959). Investigations into the mineralization pattern of human dental enamel. Part 1. Polarized light studies. *Journal of Dental Research, 39*(6), 1096-1107.

Allan, J. H. (1967). Maturation of enamel. In A. E. W. Miles (Ed.). *Structural and chemical organization of teeth,* Vol. 1 (pp. 467-494). New York: Academic Press.

Al-Mosawi, M., Davis, G. R., Bushby, A., Montgomery, J., Beaumont, J. & Al-Jawad, M. (2018). Crystallographic texture and mineral concentration quantification of developing and mature human incisal enamel. *Scientific Reports 8*, 14449 https://doi:10.1038/s41598-018-32425-y

Bakker, P. C. A. M., Kurver, P. H. J., Kuik, D. J. & Van Geijn, H. P. (2007). Elevated uterine activity increases the risk of fetal acidosis at birth. *American Journal of Obstetrics and Gynecology 196,* 313.e1.313.e6.

Bawden, J. W. (1989). Calcium transport during mineralization. *The Anatomical Record, 224*, 226-233.

Berkovitz, B. K. B., Holland, G. R. & Moxham, B. J. (1981). *A colour atlas & textbook of oral anatomy*. 2nd impression 1981, p93. London, Wolf Medical Publications Ltd. ISBN 0 7234 0719 3.

Birch, W. & Dean, M. C. (2014). A method of calculating human deciduous crown formation times and of estimating the chronological ages of stressful events

occurring during deciduous enamel formation**.** *Journal of Forensic and Legal Medicine. 22,* 127-144. http://dx.doi.org/10.1016/j.jflm.2013.12.002

Bodier-Houllé, P., Steuer, P., Voegel, J. C. & Cuisinier, F. J. (1998). First experimental evidence for human dentine crystal formation involving conversion of octacalcium phosphate to hydroxyapatite. *Acta Crystallographica Section D Biological Crystallography, 1*,54 (Pt 6 Pt 2), 1377-1381.

Boesenberg, U., Ryan, C. G., Kirkham, R., Siddons, D. P., Alfred, M., Garrevoet, J., Núñez, T., Claussen, T., Kracht, T. & Falkenberg, G. (2016). Fast X-ray microfluorescence imaging with submicrometer-resolution integrating a Maia detector at beamline P06 at PETRA III. *Journal of Synchrotron Radiation 23,* 1550-1560. https://doi.org/10.1107/S1600577516015289

Boyde, A. (1964). *The structure and development of mammalian enamel*. PhD Thesis, London: University of London

Boyde, A. (1989). Enamel. In A. Oksche & L. Vollrath (Eds.). *Handbook of microscopic anatomy,* Vol. 2, *Teeth*. (pp. 309-473). Berlin: Springer Verlag.

Boyde, A. (1997). Microstructure of enamel. In: Chadwick, D. J., Cardew, G. (Eds.). *Dental enamel. Proceedings of the Ciba Foundation Symposium 205.* (pp. 18–31), Chichester, John Wiley and Sons Inc.

Canturk, N, Atsu, S. S., Aka, S. P. & Dagalp, R. (2014). Neonatal line on fetus and infant teeth. An indicator of live birth and mode of delivery. *Early Human Development, 90,* 393-397.

Cevc, G., Cevc, P., Schara, M. & Skaleric, U. (1980). The caries resistance of human teeth is determined by the spatial arrangement of hydroxyapatite microcrystals in the enamel. *Nature, 286,* 425-286.

Colak, A., Yildiz, O., Toprak, B., Turkon, H., Halicioglu, O. & Coker, I. (2014). Correlation between calcium and phosphorus in cord blood and birth size in term infants. *Minerva Pediatrica, 68*(3), 182-188.

Crabb, H. S. M. (1959). The pattern of mineralization of human dental enamel. *Proceedings of the Royal Society of Medicine, 52,* 118-122.

Dean, C., Le Cabec, A., Spiers, K., Zhang, Y. & Garrevoet, J. (2018). Incremental distribution of strontium and zinc in great ape and fossil hominin cementum using synchrotron X-ray fluorescence mapping. *Journal of The Royal Society Interface,* 15, 20170626. http://dx.doi.org/10.1098/rsif.2017.0626

Dolphin, A. E., Goodmann, A. H. & Amarasiriwardena, D. (2005). Variation in elemental intensities among teeth and between pre- and postnatal regions of enamel. American *Journal of Physical Anthropology, 128,* 878-888

Donangelo, C. M. & King, J. C. (2012). Maternal zinc intakes and homeostatic adjustments during pregnancy and lactation. *Nutrients, 4,* 782-794 https://doi:10.3390/nu4070782

Dreosti, I. E., McMichael, A. J., Gibson, G. T., Buckley, R. A., Hartshorne, J. M. & Colley, D. P. (1982). Fetal and maternal serum copper and zinc levels in human pregnancy. *Nutrition Research, 2*, 591-602.

Du. C, Falini, G., Fermani, S., Abbott, C. & Moradian-Oldak, J. (2005). Supramolecular assembly of amelogenin nanospheres into birefringent microribbons. *Science, 307,* 1450-1454.

Eli, I., Sarnat, H. & Talmi, E. (1989). Effect of the birth process on the neonatal line in primary tooth enamel. *Pediatric Dentistry, 11,* 220-223.

Ezzo, J. A. (1994). Putting the "chemistry" back into archaeological bone chemistry analysis: Modeling potential paleodietary indicators. *Journal of Anthropological Archaeology, 13,* 1-34.

Falkenberg, G., Fleissner, G., Fleissner, G., Alraun, P., Boesenberg, U. & Spiers, K. (2017). Large-scale high resolution micro-XRF analysis of histological structures in the skin of the pigeon beak. *X-Ray Spectrom, 46,* 467–473. https://doi:10.1002/xrs.2769.

Featherstone, J. D. B. & Nelson, D. G. A. (1980). The effect of fluoride, zinc, strontium, magnesium and iron on the crystal-structural disorder in synthetic carbonated apatites. *Australian Journal of Chemistry, 33,* 2363–2368. https://doi:10.1071/CH9802363.

Gittleman, I. F., Pincus, J. B., Schmerzler, E. & Saito, M. (1956). Hypocalcemia occurring on the first day of life in mature and premature infants. *Pediatrics, 18,* 721-729.

Granstrom, G. & Linde, A. (1981). ATP-dependent uptake of Ca^{++} by a microsomal fraction from rat incisor odontoblasts. *Calcified Tissue International, 33,* 125-128.

Gustafson, A. G. (1959). A morphologic investigation of certain variations in the structure and mineralization of human dental enamel. *Odontologisk Tidskrift, 67,* 361-472.

Gustafson, G., Gustafson, A. G. (1967). Micro-anatomy and histochemistry of enamel. In A. E. W. Miles (Ed.). *Structural and chemical organization of teeth* Vol. II (pp. 75–134). New York: Academic Press.

Helwig, J. T., Parer, J. T., Kilpatrick, S. J. & Laros, R. K. (1996). Umbilical cord blood acid-base state: What is normal? *American Journal of Obstetrics and Gynecology, 174*(6), 1807-1814.

Hillson, S. (2014). *Tooth development in human evolution and bioarchaeology*. Cambridge, UK, Cambridge University Press.

Hohenauer, L., Rosenberg, T. F. & Oh, W. (1970). Calcium and phosphorus homeostasis on the first day of life. *Biology of the Neonate, 15,* 49-56.

Hubbard, M. J. (2000). Calcium transport across the dental epithelium. *Critical Reviews in Oral Biology and Medicine, 11*(4), 437-466.

Humphrey, L. T., Jeffries, T. E., Dean, M. C. (2004). Investigation of age at weaning using Sr/Ca ratios in human tooth enamel. *American Journal of Physical Anthropology Supplement* 38: 117.

Humphrey L. T., Dean, M. C. & Jeffries, T. E. (2007). An evaluation of changes in strontium/calcium ratios across the neonatal line in human deciduous teeth. In (S. E. Bailey, J-J. Hublin (Eds.). *Dental Perspectives on Human Evolution: State of the Art Research in Dental Paleoanthropology* (pp. 303–319). Dordrecht, Springer.

Humphrey, L. T., Jeffries, T. E. & Dean, M. C. (2008a). Micro spatial distributions of lead and zinc in human deciduous tooth enamel. In J. D., Irish, G. C. Nelson, (Eds.). *Technique and Application in Dental Anthropology, Studies in Biological Anthropology* (pp. 87-110). Cambridge University Press.

Humphrey, L. T., Dirks, W., Dean, M. C. & Jeffries, T. E. (2008b). Tracking dietary transitions in weanling baboons (*Papio hamadryas anubis*) using strontium/calcium ratios in enamel. *Folia Primatologica* 79; 197-212. https://doi:10.1159/000113457

Humphrey, L. T., Dean, M. C., Jeffries, T. E. & Penn, M. (2008b). Unlocking evidence of early diet from tooth enamel. *Proceedings of The National Academy of Sciences USA, 105,* 6834–9. https://doi:10.1073/pnas.0711513105.

Humphrey, L. T. (2009). Weaning behaviour in human evolution. *Seminars in Cell and Developmental Biology, 21,* 453–461.

Humphrey, L. T. (2014). Isotopic and trace element evidence of dietary transitions in early life. *Annals of Human Biology, 41*(4), 348–57. https://doi:10.3109/03014460.2014.923939.

Hurnanen, J., Visnapuu, V., Sillanpää, M., Löyttyniemi, E. & Rautava, J. (2016). Deciduous neonatal line: Width is associated with duration of delivery. *Forensic Science International, 271,* 87-91.

Hsu, S. C. & Levine, M. A. (2003). Perinatal calcium metabolism: physiology and pathophysiology. *Seminars in neonatology 9,* 23-36.

Jakobsen, J. (1975). Neonatal lines in human dental enamel. Occurrence in first permanent molars in males and females. *Acta Odontologica Scandinavica, 33,* 95-105.

Janardhana, M., Umadethan, B., Biniraj, K. R., Vinod Kumar, R. B. & Rakesh, S. (2011). Neonatal line as a linear evidence of live birth: Estimation of postnatal

survival of a new born from primary tooth germs. *Journal of Forensic Dental Science, Jan-Jun 3*(1), 8-13.

Johnson, N. W. (1971). Factors affecting the differential dissolution of human enamel in acid and EDTA. A scanning electron microscope study. *Archives of Oral Biology, 16,* 385-396.

Keinan, D., Smith, P. & Zilberman, U. (2006). Microstructure and chemical composition of primary teeth in children with Down syndrome and cerebral palsy. *Archives of Oral Biology, 51,* 836-843.

Keinan, D., Smith P. & Zilberman, U. (2007). Prenatal growth acceleration in maxillary deciduous canines of children with Down syndrome: histological and chemical composition study. *Archives of Oral Biology, 52,* 961-966.

Kim, T. H., Bae, C. H., Lee, J. C., Kim, J. E., Yang, X., de Crombrugghe, B. & Cho E. S. (2015). Osterix regulates tooth root formation in a site-specific manner. *Journal of Dental Research, 94*(3), 430-438.

Kirkham, R., Dunn, P. A., Kuczewski, A. J., Siddons, D. P., Dodanwela, R. & Moorhead, G. F. (2010). The Maia Spectroscopy Detector System: Engineering for Integrated Pulse Capture, Low-Latency Scanning and Real-Time Processing. *AIP Conference Proceedings 1234,* 240–3. https://doi:10.1063/1.3463181.

Klimuszko, E., Orywal, K., Sierpinska, T., Sidum, J. & Golebiewska, M. (2018). The evaluation of zinc and copper content in tooth enamel without any pathological changes – an in vitro study. *International Journal of Nanomedicine, 13,* 1257-1264.

Kodaka, T. & Higashi, S. (1995). Incremental lines of human enamel observed by scanning electron microscopy: Review. *Archives of Comparative Biology of Tooth Enamel, 4,* 53-58.

Kodaka, T., Sano, T. & Higashi, S. (1996). Structural and calcification patterns of the neonatal line in the enamel of human deciduous teeth. *Scanning Microscopy, 10*(3), 737-743, discussion 743-4.

Kovacs, C. (2011). Fetal mineral homeostasis. In F. H. Glorieux, J. M. Pettifor & H. Jüppner (Eds.). *Pediatric bone: Biology and Disease*, *2nd edition* (pp. 247-275). San Diego: Elsevier/Academic.

Kronfeld, R. & Schour, I. (1939). Neonatal dental hypoplasia. *Journal of The American Dental Association, 26,* 18-32.

Krukowski, M., & Smith, J. J. (1976). pH and the level of calcium in the blood of fetal and neonatal albino rats. *Biology of the Neonate, 29,* 148-161.

Kurek, M., Żądzińska, E., Sitek, A., Borrowska-Strugińska, B., Rosset, I. & Lorkiewicz, W. (2015). Prenatal factors associated with neonatal line thickness in human deciduous incisors. HOMO – *Journal of Comparative Human Biology, 66,* 251-263.

Lacruz, R. S., Nanci, A., Kurtz, I., Wright, T. J. & Paine, M. L. (2009). Regulation of pH during amelogenesis. *Calcified Tissue International, 86*(2), 91-103 https://doi10.1007/s00223-009-9326-7.

LeGeros, R. Z. (1981). Apatites in biological systems. *Progress in Crystal Growth and Characterization of Materials, 4,* 1-46.

LeGeros, R. Z., Bleiwas, C. B., Retino, M., Rohanizadeh, R. & LeGeros, J. P. (1999). Zinc effect on the in vitro formation of calcium phosphates: *Relevance to clinical inhibition of calculus formation. American Journal of Dentistry, 12*(2), 65-71.

Lingawi, H., Barbour, M., Lynch, R. J. M. & Anderson, P. (2011). Effect of zinc ions (Zn^{2+}) on hydroxyapatite dissolution kinetics studied using scanning microradiography. *Caries Research, 45*, 174-242 abstracts, p. 195 number 51.

Lochner, F., Appleton, J., Keenan, F., & Cooke, M. (1999). Multi-element profiling of human deciduous teeth by laser ablation-inductively coupled plasma-mass spectrometry. *Analtica Chimica Acta 401,* 299–306.

Lu, Y., Papagerakis, P., Yamakoshi, Y., Hu, J. C-C., Bartlett, J. D. & Simmer, J. P. (2008). Functions of KLK4 and MMP-20 in dental enamel formation. *Biological Chemistry, 389*(6), 695-700. https://doi:10.1515/BC.2008.080

Macchiarelli, R. & Bondioli, L. (2000). Multimedia dissemination of the "Isola Sacra" human paleobiological project: reconstructing lives, habits, and deaths of the "ancient Roman people" by means of advanced investigative methods. In A. Guarino (Ed.), *Proceedings of 2nd International Congress on Science and Technology for the Safeguard of Cultural Heritage in the Mediterranean Basin*, vol. 2, (pp.1075-1080). Paris: Elsevier.

Martin, R. R., Naftel, S. J., Nelson, A. J., & Sapp, W. D. III. (2007). Comparison of the distributions of bromine, lead, and zinc in tooth and bone from an ancient Peruvian burial site by X-ray fluorescence. *Canadian Journal of Chemistry, 85,* 831–836. https://doi:10.1139/v07-100.

Mayer, I., Apfelbaum, F. & Featherstone, J. D. B. (1994). Zinc ions in synthetic carbonated hydroxyapatites. *Archives of Oral Biology, 39,* 87–90. doi:10.1016/0003-9969(94)90040-X.

Meites, S. (1975). Normal Total Plasma Calcium in the Newborn, *CRC Critical Reviews in Clinical Laboratory Sciences, 6*(1), 118, https:// doi:10.3109/10408367509151562

Mishra, S., Thomas, H. F., Fearne, J. M., Boyde, A. & Anderson, P. (2009). Comparison of demineralization rates in pre- and postnatal enamel and at the neonatal line. *Archives of Oral Biology, 54s*, s101-s106.

Mohammed, N. R., Mneimne, M., Hill, R. G., Al-Jawad, M., Lynch, R. J. M. & Anderson, P. (2014). Physical chemical effects of zinc on in vitro enamel

demineralization. *Journal of Dentistry, 42,* 1096–1104. https://doi:10.1016/j.jdent.2014.04.014.

Mortimer, K. V. (1970). The relationship of deciduous enamel structure to dental disease. *Caries Research, 4,* 206-223.

Müller, W., Nava, A., Evans, D., Rossi, P. F., Alt, K. W. & Bondioli, L. (2019). Enamel mineralization and compositional time-resolution in human teeth evaluated via histologically-defined LA-ICPMS profiles. *Geochimica et Cosmochimica Acta,* (in press).

Nava, A., Bondiolli, L., Coppa, A., Dean, C., Rossi, P.A., Zanolli, C. (2017) New regression formula to estimate the prenatal crown formation time of human deciduous central incisors derived from a Roman Immperial sample (Velia, Salerno, Italy, I-II cent. CE). *PLoS ONE 12(7):* e0180104. https://doi. org/10.1371/journal.pone.0180104

Nava, A., Frayer, D. W. & Bondioli, L. (2019). Longitudinal analysis of the microscopic dental enamel defects of children in the Imperial Roman community of *Portus Romae* (necropolis of Isola Sacra, 2nd to 4th century CE, Italy). *Journal of Archaeological Science: reports 23,* 406-415. https://doi.org/10.1016/j.jasrep.2018.11.007

Neville, M. C. & Watters, C. D. (1983). Secretion of calcium into milk: Review. *Journal of Dairy Science, 66*(3), 371-380.

Okada, M. (1943). Hard tissues of animal body: highly interesting details of Nippon studies in periodic patterns of hard tissues are described. Shanghai Evening Post, Special Edition, health, recreation and medical progress, pp. 15–31.

Ofakunrin, A. O. D., Collins, J., Diala, U. M., Afolaranmi, T. O. & Okolo, S. N. (2017). Relationship between maternal serum zinc, cord blood zinc and birth weight for term newborn infants in Jos, Plateau State, Nigeria. *Jos Journal of Medicine, 11*(2), 12-20.

Ranggård, L., Norén, J. G. & Nelson, N. (1994). Clinical and histologic appearance in enamel of primary teeth in relation to neonatal blood ionized calcium values. *Scandinavian Journal of Dental Research, 102,* 254-259.

Robinson, C. (2014). Enamel maturation: a brief background with implications for some enamel dysplasias. *Frontiers in Physiology, Craniofacial Biology, article 388 vol 5,* 1-6. https://doi:10.3389/fphys.2014.00388

Robinson, C., Brookes, S. J., Bonass, W. A., Shore, R. C., Kirkham, J. (1997). Enamel maturation. In: Chadwick, D. J., Cardew, G. (Eds.). *Dental enamel. Proceedings of the Ciba Foundation Symposium 205.* (pp. 118–134), Chichester, John Wiley and Sons Inc.

Rosser, H., Boyde, A., Stewart, A. D. G. (1967). Preliminary observations of the calcium concentration in developing enamel assessed by scanning electron-probe X-

ray emission microanalysis. *Archives of Oral Biology, 12,* 431–440. https://doi:10.1016/0003-9969(67)90018-0

Rossipal, E., Krachler, M., Li, F. & Micetic-Turk, D. (2000). Investigation of the transport of trace elements across barriers in humans: studies of placental and mammary transfer. *Acta Paediatrica, 89,* 1190-1195.

Rushton, M. A. (1933). Fine Contour Lines of Enamel of Milk Teeth. *Dental Record 53,* 170-175.

Rushton, M. A. (1939). The birefringence of deciduous tooth enamel formed before and after birth. *British Dental Journal, 67,* 1–10.

Sabel, N., Johansson, C., Kühnisch, J., Robertson, A., Steiniger, F., Norén, J. G., Klingberg, G. & Nietzsche, S. (2008). Neonatal lines in the enamel of primary teeth – A morphological and scanning electron microscopic investigation. *Archives of Oral Biology, 53,* 954-963.

Sánchez-Quevedo, M. C., Crespo, P. V., García, J. M. & Campos, A. (1992). X-ray histochemistry of zinc in dental tissues. *European Archives of Biology 103,* 47–49.

Schour, I. (1936). The neonatal line in the enamel and dentine of the human deciduous teeth and first permanent molar. *Journal of The American Dental Association 23,* 1946-1955.

Schroer, C. G. et al. (2010) Hard X-ray nanoprobe at beamline P06 at PETRA III. *X-Ray Mirror 616,* 93–97. https://doi:10.1016/j.nima.2009.10.094.

Silvestre, D., Martìnez-Costa, C., Lagarda, J. M., Brines, J., Farré, R. & Clemente, G. (2001). Copper, iron and zinc contents in human milk during the first three months of lactation. A longitudinal study. *Biological Trace Element Research, 80,* 1-11.

Silness, J. (1969). Some variations in the microradiographic appearance of human deciduous enamel. *Odontologica Revy, 20,* 93-110.

Simmons, L. M., Montgomery, J., Beaumont, J., Davis, G. R., Al-Jawad, M. (2013). Mapping the spatial and temporal progression of human dental enamel biomineralization using synchrotron X-ray diffraction. *Archives of Oral Biology, 58,* 1726-1734.

Skaleric, U., Ravnik, C., Cevc, P., Schara, M. (1982). Microcrystal arrangement in human deciduous dental enamel studied by electron paramagnetic resonance. *Caries Research, 16,* 47-50.

Skinner, M., & Dupras, T. (1993). Variation in birth timing and location of the neonatal line in human enamel. *Journal of Forensic Sciences, 38*(6), 1388-1390.

Sognnaes, R. F. (1949). The organic elements of the enamel III. The pattern of the organic framework in the region of the neonatal and other incremental lines of the enamel. *Journal of Dental Research, 28,* 558-564.

Stenger, V., Eitzman, D., Anderson, T., De Padua, C., Gessner, I. & Prystowsky, H. (1964). Observations on the placental exchange of the respiratory gases in pregnant women at cesarean section. *American Journal of Obstetrics and Gynecology, 88,* 45-57.

Stock, S. R., Veis, A., Telser, A. & Cai, Z. (2011). Near tubule and intertubular bovine dentin mapped at the 250 nm level. *Journal of Structural Biology, 176,* 203–11. https://doi:10.1016/j.jsb.2011.07.014.

Stock, S. R., Deymier-Black, A. C., Veis, A., Telser, A., Lux, E. & Cai, Z. (2014). Bovine and equine peritubular and intertubular dentin. *Biomineralization, 10,* 3969–3977. https://doi:10.1016/j.actbio.2014.05.027.

Stock, S. R., Finney, L. A., Telser, A., Maxey, E., Vogt, S. & Okasinski, J. S. (2017). Cementum structure in Beluga whale teeth. *Acta Biomaterialia, 48,* 289-299. http://dx.doi.org/10.1016/j.actbio.2016.11.015

Sun, Y., Gleber, S-C., Jacobsen, C., Kirz, J., & Vogt, S. (2015). Optimizing detector geometry for trace element mapping by X-ray fluorescence. *Ultramicroscopy 152,* 44–56. https://doi:10.1016/j.ultramic.2014.12.014.

Terrin, G., Canani, R. B., Chiara, M. Di., Pietravalle, A., Aleandri, V., Conte, F. & De Curtis, M. (2015). Zinc in early life: A key element in the fetus and preterm neonate. *Nutrients, 7,* 10427-10446. https://doi:10.3390/nu7125542

Thomas, H. F. & Lee, D. (2003). Relative amounts of pre-natal and postnatal enamel in human primary incisors. *Journal of Dental Research, IADR Abstract number 1188*.

Wasowicz, W., Gromadzinska, J., Szram, K., Rydzynski, K., Cieslak, J. & Pietrzak, Z. (2001). Selenium, zinc, and copper concentrations in the blood and milk of lactating women. *Biological Trace Element Research, 79,* 221-233.

Webber, D. F. & Eisenmann, D. R. (1971). Microscopy of the neonatal line in developing human enamel. *American Journal of Anatomy, 132,* 375-392.

Whittaker, D. K. & Richards, D. (1978). Scanning electron microscopy of the neonatal line in human enamel. *Archives of Oral Biology, 23,* 45-50.

Willson, P. R. & Beynon, A. D. (1989). Mineralization differences between human deciduous and permanent enamel measured by quantitative microradiography. *Archives of Oral Biology, 34*(2), 85-88.

Witzel, C. (2014). Echoes from birth – Mutual benefits for physical and forensic anthropology by applying increment counts in enamel of deciduous teeth for ageing. *Anthropologischer Anzeiger, 71,* 87–103.

Zanolli, C., Bondioli, L., Manni, F., Rossi, P. & Macchiarelli, R. (2011). Gestation length, mode of delivery and neonatal line thickness variation. *Human Biology, 83*(6), 695-713.

Żądzińska, E., Kurek, M., Borowska-Struginska, B., Lorkiewicz, W., Rosset, I. & Sitek, A. (2013). The effect of the season of birth and of selected maternal factors on linear enamel thickness in modern human deciduous incisors. *Archives of Oral Biology, 58,* 951-963.

Figures

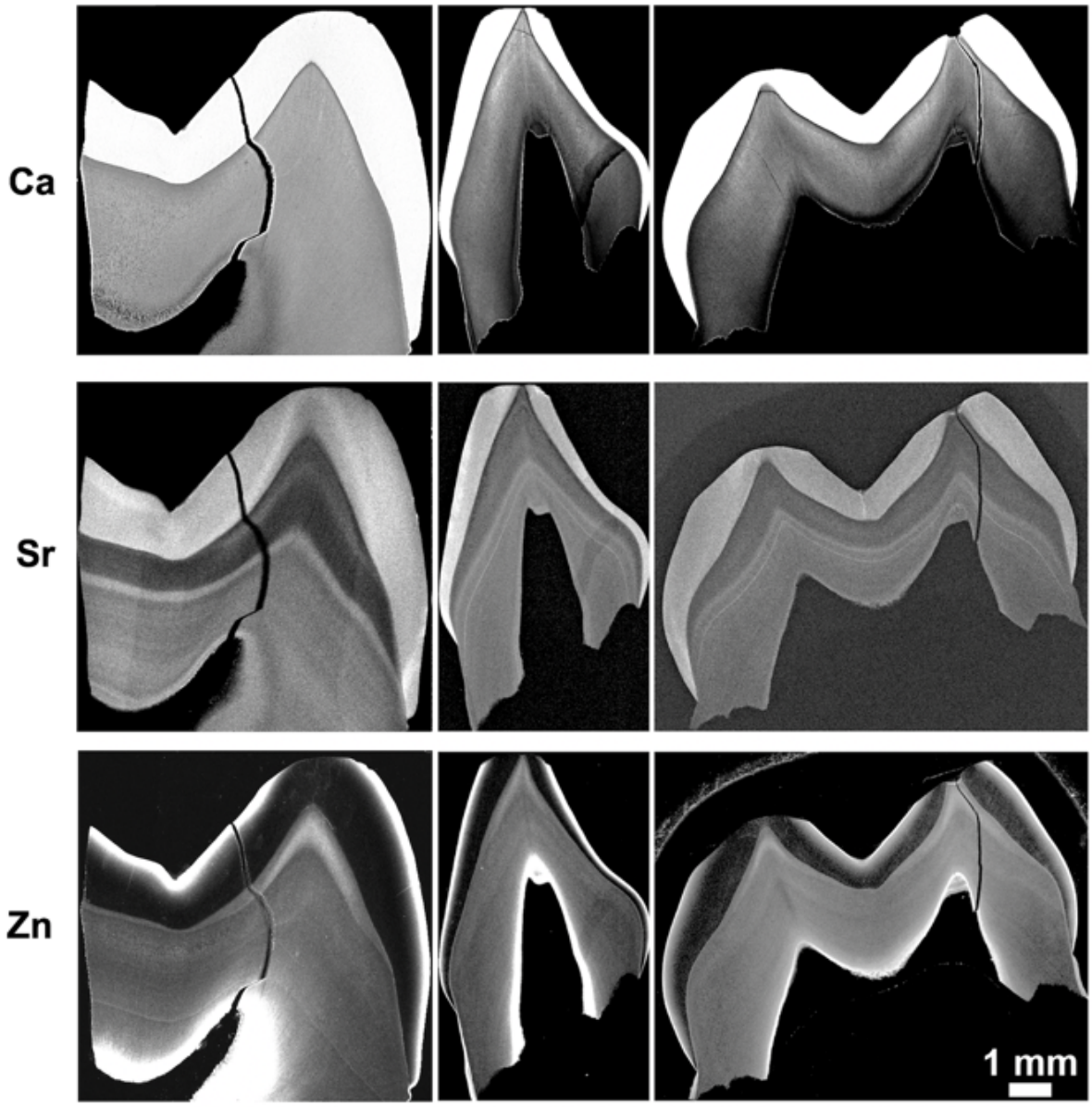

Figure 1

SXRF overview maps for calcium, strontium and zinc of three deciduous teeth. The deciduous upper second molar to the left in from one individual and the deciduous lower canine and upper second molar to the right are both from a second individual. Scans were acquired at 10 µm resolution and 10 ms integration time.

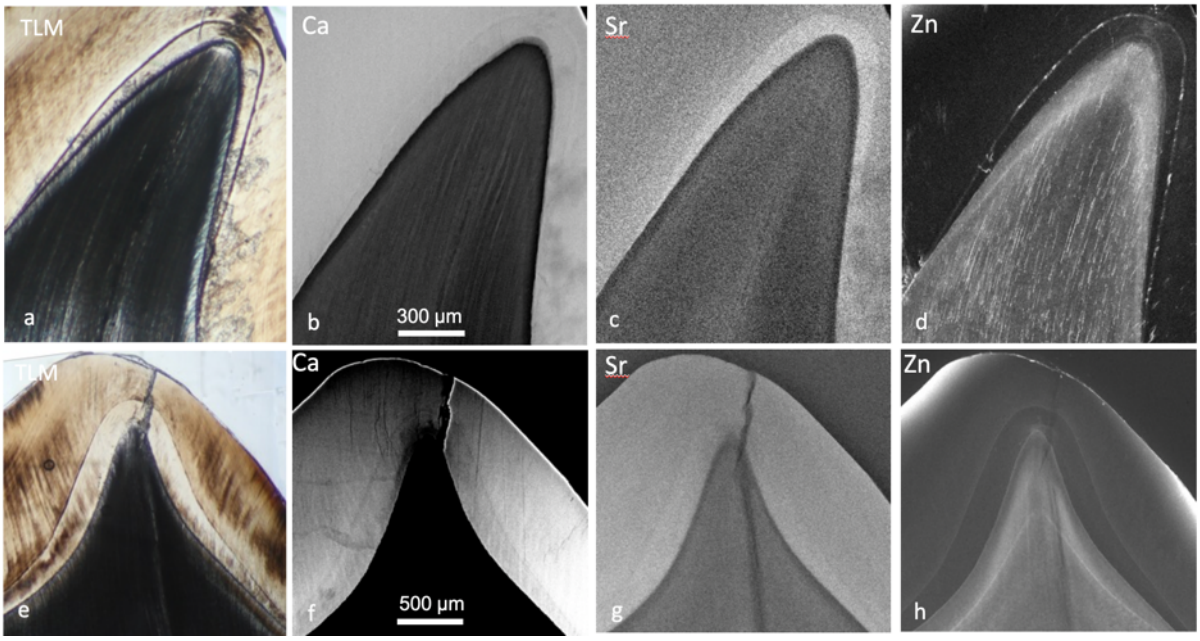

Figure 2

Transmitted light micrographs (TLM) of the NNL in an upper deciduous second molar (a) and an lower deciduous second molar cusp (e) together with SXRF maps of Ca, Sr and Zn for the same field of view. Scans were acquired at 2.5 µm resolution and 10 ms integration time.

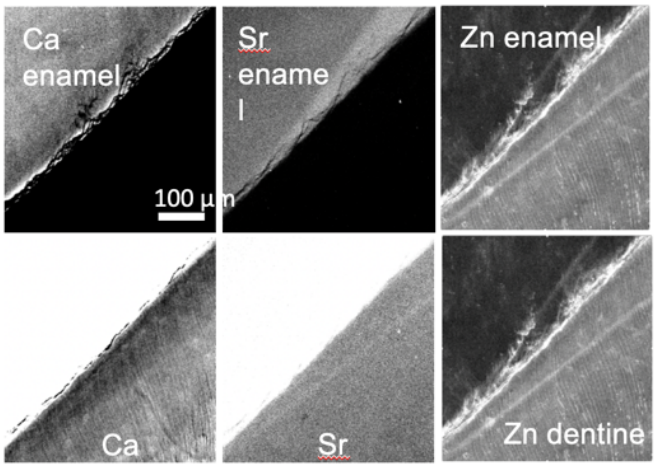

Figure 3

SXRF maps of Ca, Sr and Zn distribution close to the EDJ in a lower deciduous canine where the NNL in enamel and dentine are converging. The image contrasts are optimised for enamel on the top row and dentine on the bottom row. Scans were acquired at 1.0 µm resolution and 10 ms integration time.

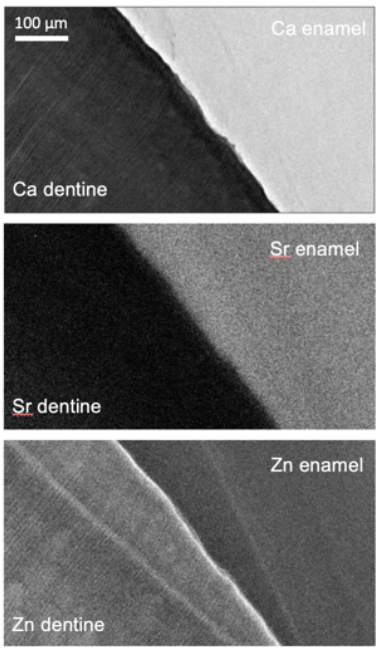

Figure 4

SXRF maps of Ca, Sr and Zn distribution at the EDJ in an upper deciduous second molar at a position where the NNL in enamel and dentine are converging. Scans were acquired at 1.0 µm resolution and 10 ms integration time.

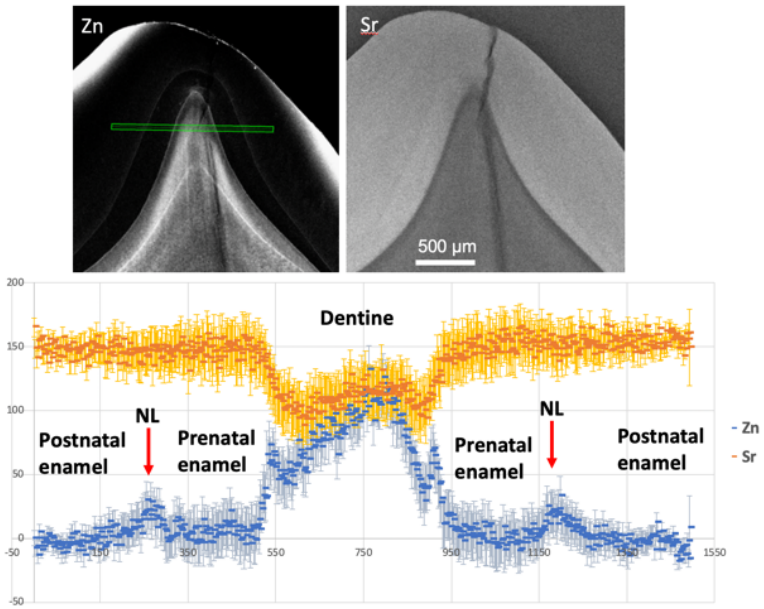

Figure 5

SXRF map of Zn and Sr in the same upper deciduous second molar cusp illustrated in Figure 2a-d. The green bar indicates the plane of the concentration plots for Zn and Sr in the graph. Error bars on the individual box plots are 2SD.

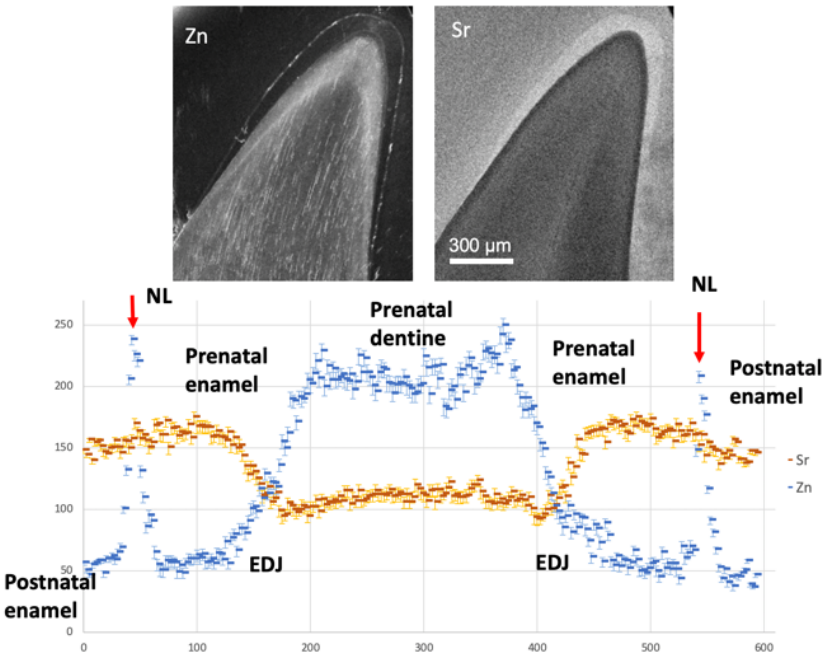

Figure 6

SXRF map of Zn and Sr in the same lower deciduous second molar cusp illustrated in Figure 2e-h. The green bars [(a) and(b)] indicate the planes of the concentration plots for Zn and Sr in the graphs [(a) and(b)]. Error bars on the individual box plots are 2SD.

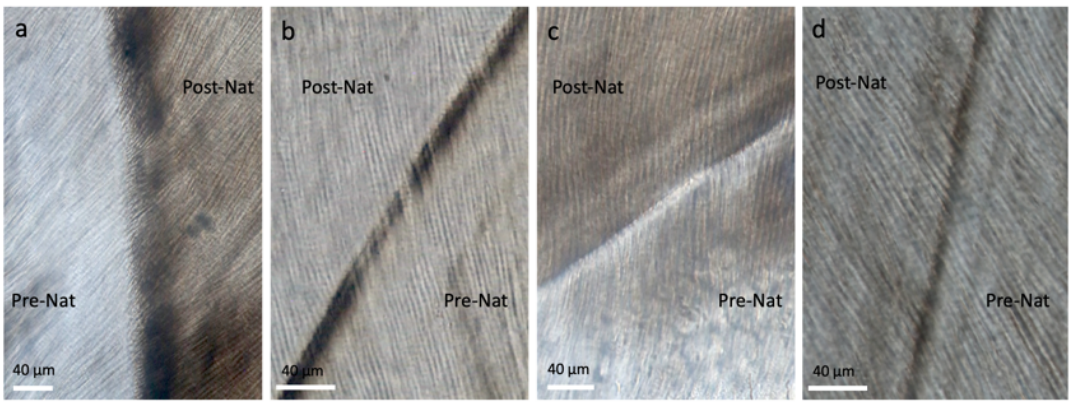

Figure 7

Transmitted light micrographs of the NNL in the enamel of some of the teeth used in this study showing the variation in width, intensity and morphology as well as the difference in appearance between pre- and postnatal enamel. Images (a) and (c) are from different cusps and different locations along the NNL in the same deciduous second molar tooth.